Chem Soc Rev

Cite this: *Chem. Soc. Rev.*, 2011, **40**, 5347–5360

www.rsc.org/csr

TUTORIAL REVIEW

Mesocrystals: Syntheses in metals and applications

Jixiang Fang,*[a] Bingjun Ding[a] and Herbert Gleiter[b]

Received 16th February 2011
DOI: 10.1039/c1cs15043j

Self-assembly of nanoparticles has emerged as a powerful technique to integrate nanoparticles into well-defined ensembles with collective properties that are different from those of individual nanoparticles and bulk materials with the same chemical composition. Compared with the classical ion/molecule-mediated crystal growth, particle-mediated crystallographically ordered self-assembly is considered as "non-classical crystallization" and the resultant product is termed a "mesocrystal". In this *tutorial review*, we begin by summarizing the progresses of this field during last decade. Secondly, we outline developments in related fields such as grain rotation and oriented attachment as well as mesocrystals. Thridly, the recent progress in the syntheses of mesocrystals particularly in metals, and the related properties are introduced. Finally, some of the current open questions are discussed.

1. Introduction

Nanomaterials, characterized by having at least one dimension between 1 and 100 nm, may display unique effects such as size effects, shape effects, surface effects, interface effects, structural effects, *etc*. Accordingly, they may exhibit a range of remarkable properties in catalysis, electronics, information storage, magnetism, *etc*. These novel properties and the resulting conceivable technological applications of nanomaterials are determined by a series of physical parameters that may include their size, shape, chemical composition, morphology, topography as well as their atomic structure (*e.g*., their crystallinity). In recent years, the successful synthesis of a great number of nanomaterials with a variety of well-defined physical parameters *via* various physicochemical routes has been reported.[1] Among these approaches to synthesize nanomaterials, the solution-phase method is a very robust one to tailor physical parameters as mentioned above hence the related properties. The exact control of physical parameters is primarily achieved by means of a solution reaction *via* the soft or hard templates, reagent chemisorption, and minimization of

[a] *State Key Laboratory for Mechanical Behavior of Materials, MOE Key Laboratory for Nonequilibrium Synthesis and Modulation of Condensed Matter, School of Science, Xi'an Jiaotong University, Shaan Xi, 710049, People's Republic of China. E-mail: jxfang@mail.xjtu.edu.cn; Tel: +86-29-82665995*
[b] *Karlsruhe Institut für Technologie (KIT), Institut für Nanotechnologie, Karlsruhe 76021, Germany*

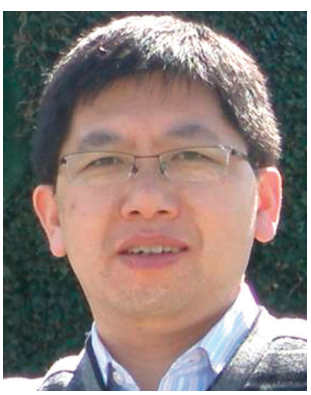

Jixiang Fang

Jixiang Fang was born in 1976 in LiaoNing, China. He received his PhD (2007, under the supervision of Professor B. J. Ding) in Materials Science at Xi'an Jiaotong University, China. He then spent one year as a postdoctoral fellow at the Institute of Nanotechnology (INT), Karlsruhe Institute of Technology (KIT) in Germany. In 2009, he worked with Prof. H. Gleiter as an Alexander-von-Humboldt scholar in INT (KIT). In 2010, he took up an appointment with a Professor of Materials Physics at Xi'an Jiaotong University. Now he is a "Tengfei" chair professor. His research has involved crystal growth, electrochemical deposition, optical properties of nanocrystals and mechanical properties of nanoamorphous materials.

Bingjun Ding

Bingjun Ding was born in 1946. He received his BS and PhD in Materials Science and Engineering from Xi'an Jiaotong University in 1981 and 1990, respectively. In 1993 he worked in a High Temperature Laboratory at the University of Minnesota as a Senior Visiting Scholar. He was the Editor-in-Chief of the book entitled "Nanostructured Materials" published by China Machine Press in 2004. Now he is a Professor for Advanced Materials in the State Key Laboratory for Mechanical Behavior of Materials, Xi'an Jiaotong University, Shaanxi Province, China. His research interests include electrical contact materials, vacuum arcs and their applications, plasma coatings and nanostructured materials.

surface energy of crystallographic facets (*i.e.*, by utilizing the Wulff's theorem).

In the previous literature, the resulting physical parameters, *e.g.*, the shape or the morphology of the crystallized structures were interpreted by means of the classical crystallization models.[2] The classical atom-mediated crystallization process starts from the aggregation of primary building blocks like atoms, ions or molecules, and forms so-called critical crystal nuclei. These nuclei grow further *via* classical atom-by-atom (or ion/molecule) attachment. The same materials can exhibit different crystal shapes or morphologies, albeit the shape of inorganic crystals is often related to the intrinsic nuclei structure. This feature is partially determined by different surface energies of crystal surfaces with different crystallographic orientations. On the other hand, the growth conditions, *e.g.*, the growth rate of a crystal face, may also significantly influence the final morphology if the same growth mechanism applies. Crystal faces with high surface energies exhibit the fastest growth rates. As a consequence, they are minimized or even disappear in the final morphology. This is the classical Wulff's rule which determines the equilibrium morphology of a crystal as being given by the minimum surface energy of all exposed crystal faces.[3] However, this purely thermodynamic model is not able to predict the correct crystal morphology in all cases, particularly in a kinetic driving system.

Recently, a new growth mechanism, *i.e.* the non-classical particle-mediated crystallization pathway was deduced by Cölfen *et al.* from biomineralization processes.[4] This mechanism is based on an oriented attachment mechanism (OA)[5] and a grain rotation process.[6] This particle-by-particle growth process always involves the oriented attachment and/or grain rotation of the building units and results in the formation of so-called "mesocrystals" *via* the mesoscale transformation. Mesocrystals are ordered mesoscale superstructures composed of individual nanocrystals that are aligned along a common crystallographic direction, exhibiting scattering properties similar to the ones of a single crystal.[7] With the appearance of the mesocrystal concept, attention has been directed toward the investigations in various systems. The mesoscale transformation process seems to be relevant in many cases: for example, Ag_2O,[8] Cu_2O,[9] ZnO,[10] TiO_2,[11] $AgInWO_4$[12,13] Calcium carbonate,[14,15] PdSe,[16] even in pure metals, Au[17] and Ag.[18,19]

In previous review papers, the syntheses of mesocrystals in oxides and various compounds had been reported.[20–22] However, the corresponding reviews for metallic materials and the related properties, in particular those originating from the mesostructures, were quite rare. In fact, owing to the unique structural characteristics, *e.g.*, the tunable surface roughness and topography, the small size of their building blocks (in the 10 nm range) as well as the high level of internal porosity, mesocrystals are well suited for many applications such as catalysts, sensors, and optical devices. In sensor applications, the sensitivity of the materials may be modified by the packing style of atoms. For example, ZnO colloidal clusters, owing to abundant inter-cluster porosity and internal surface area, possess a high concentration of surface and subsurface oxygen vacancies, which result in a strong green-yellow emission and high sensitivity for humidity measurements at room temperature.[10] In this tutorial review, we briefly summarize the history of the particle-mediated *meso*-assembly, describe the recent advancements and achievements made on the syntheses of metallic mesocrystals, illustrate the properties and applications of the mesostructures, but not limited to metals owing to relative reports are just emerging, and finally discuss our predictions for further development in this field.

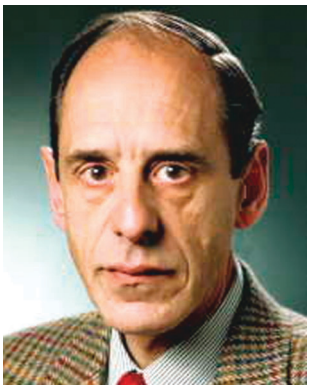

Herbert Gleiter

Herbert Gleiter was born in 1938. He obtained his PhD in 1966 in physics from the Max Planck Institute of Materials Science and the University of Stuttgart. After working for several years as a research fellow at Harvard University and MIT, he accepted positions as director of the Institute of Materials Physics at the Universities of Bochum, Saarbrücken, the ETH (Swiss Federal Institute of Technology) Zürich, and the University of Hamburg–Harburg. In 1994, the government of Germany appointed him to the Executive Board of the Research Center Karlsruhe, Germany's largest national laboratory. Four years later, he initiated (together with Noble Laureate J.M. Lehn and D. Fenske) the Institute of Nanotechnology (INT) at the Research Center Karlsruhe. Today, the INT is Germany's largest research institute in the area of nanotechnology. He is a member of the National Academy of Sciences of Germany, the United States National Academy of Engineering, the American Academy of Arts and Sciences, the European Academy of Sciences, and the Indian National Academy of Engineering.

2. History

2.1 Grains rotation

In the early 1970s, a considerable amount of experimental and theoretical evidence was presented, suggesting that the structures and properties of grain boundaries in metals depend on the orientation relationships between the boundaries and the boundary inclination. In particular, a number of special misorientations have been identified that result in boundaries with special properties such as low energy. These boundaries are frequently referred to as "special boundaries". To verify the existence of these special boundaries, several models[23] on grain boundary and experimental evidences[24] were reported. An experiment designed by Herrmann *et al.* was applied to validate the proposed grain boundary models by comparing the predicted and the experimentally observed boundaries of low energy. The experiment is displayed in Fig. 1.[24] The energy–misorientation relationship of grain boundaries in copper and several other materials was measured by recording the rotation of a single crystal sphere of copper sintered on a flat single crystal (Fig. 1a and b). The crystal lattices of the spheres and the plate were randomly misoriented at the initial stage. A rotation of the copper ball was achieved by the indicated diffusive flux of atoms, conveying a wedge shaped

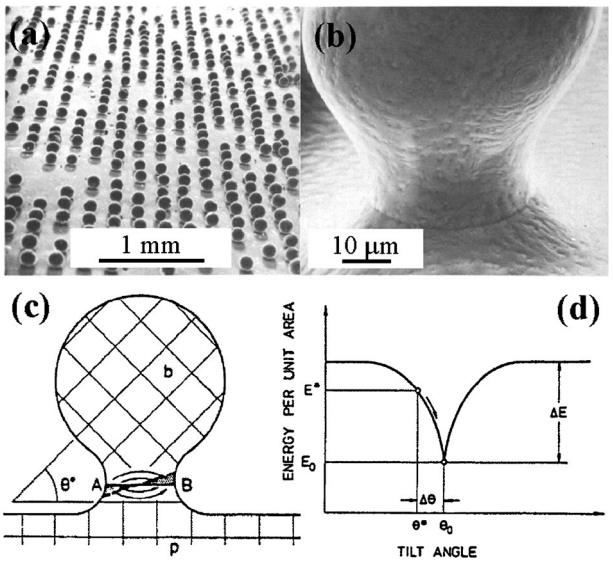

Fig. 1 (a) SEM image showing the lateral arrangement of the single crystal copper balls on the single crystal copper plate. (b) An individual ball sintered onto the plate. (c) Schematic diagram showing a grain boundary formed by sintering a ball onto a plate. The crystal lattices of the ball and the plate are misorientated initially. A rotation of the ball may be achieved by the indicated diffusive flux of atoms removing a wedge shaped piece of material from the left part of the boundary and inserting it into the right part. (d) Schematic curve of the grain boundary energy per unit area *versus* tilt angle. Ref. 24, copyright 1976, reproduced with permission from Elsevier.

piece of material from the left part of the boundary into the right part (Fig. 1c). The results suggested that low-energy boundaries may exist at non-high-coincidence orientation relationships. The shape of the energy–misorientation curve in the vicinity of an energy cusp might have the shape of a trough or a "V" with an obtuse angle at the tip (Fig. 1d). The observations supported a grain boundary model based on a periodic arrangement of structural units.[23]

In the following decades, grain-boundary curvature-driven grain growth in polycrystalline materials was extensively studied, contributing to a new growth mechanism: grain-rotation-induced grain coalescence.[25] According to this mechanism, the rotation of grains among neighboring grains results in a coherent grain–grain interface (the grains share the same crystallographic orientation), which leads to the coalescence of neighboring grains *via* the elimination of common grain boundaries, thus forming a single larger grain.

It is noted that a similar experiment with the one designed by H. Gleiter's group (Fig. 1) was carried out by Yeadon *et al.* in 1998 on a length scale of several orders of magnitude smaller for Ag nanoparticles (5–20 nm in diameter) deposited onto clean Cu.[26] They observed a process called "contact epitaxy". The Ag nanocrystals were initially randomly oriented but subsequently aligned epitaxially with the substrate. Once aligned with the substrate, the nanocrystals were also aligned with each other. In a series of simulations, Averback *et al.* showed that the process may occur as follows.[26] After the nanocrystals have "landed" on the substrate, the stress between the nanocrystals and the substrate creates a dislocation within the nanoparticle. As this dislocation moves toward the nanocrystal surface, the particle "rotates", resulting in full alignment with the substrate.

2.2 Oriented attachment

The understanding of the physics involved in the formation of a nanocrystal is of fundamental interest. According to the traditional models, individual atoms or molecules are added or subtracted as the crystal grows or shrinks. Crystal coarsening has been described in terms of the growth of large particles at the expense of small particles, driven by surface energy reduction. This is called Ostwald ripening (OR). In 1998, based on the observations of coarsening processes during the hydrothermal synthesis of anatase TiO_2 nanocrystals,[27] Penn and Banfield proposed a new class of crystallization mechanism, in which the natural minerals also grow through a process of "oriented attachment" (OA) of nanocrystals. The so-called oriented attachment mechanism describes the spontaneous self-organization of adjacent particles, so that they share a common crystallographic orientation, followed by the joining of these particles at a planar interface. The process is particularly relevant in the nanocrystalline regime, where bonding between the nanoparticles reduces the overall energy by decreasing the surface energy associated with unsatisfied bonds. This observation is very important for the creation of advanced artificial materials.

2.2.1 OA and OR. Since the classical OR model of particle coagulation was renewed by the proposal of OA growth mechanism to explain deviations between experimental results and theoretical models, several studies have been devoted to investigate their correlations during the coarsening of nanoparticles. For example, kinetic models were developed for various systems such as multistep models or collision models in liquid suspension, air, or vacuum or on free surfaces. Although the resulting theoretical models cannot yet account for all experimental observations, the proposed process seems to be common to most experiments.

By means of calculating the average particle sizes and the observation *via* the transmission electron microscopy (TEM), Huang[28] and coworkers found that OA and OR crystal growth mechanisms occurred simultaneously.[29] In the early stages of the crystal growth, OA mechanism may occur predominantly. With an extended reaction time, OR can, to some extent, play an important role to assist the process of OA in forming final single crystals. These results are consistent with the observation in our previous experiments upon the conversion from silver dendritic mesocrystals to single crystals.[30]

The morphologies and structures of the products depend on the different operating mechanisms of OA or OR. Twins, dislocations and stacking faults are frequently observed when a growth process is dominated by the OA mechanism. The growth of these defects is in line with the predicaton in OA-based growth involving the assembly of microstructurally different particles. In addition to the structural defects, OA may also result in irregular and rough surfaces owing to particle-by-particle aggregation, while OR prefers to remove the irregularities arising from OA and hence tends to yield rounded and smooth particles if it operates simultaneously with OA.[30] Furthermore, after the OA step, the loose "raw" structures

aggregated *via* the OA mechanism may also be further crystallized and gradually transformed into densely packed ones through OR processes. In addition, with the assistance of surfactants or the intrinsic crystal structure, the OA mechanism can be a more effective way of producing anisotropic morphologies. In contrast, OR seems to create the isotropic structures by the dissolution/precipitation of ions in solution.

2.2.2 OA and grain rotation. As described above, grain-rotation-induced grain coalescence in polycrystalline bulk materials has been widely investigated up to now. In fact, grain rotation in nanometre-sized grains in solution may be significantly easy in comparison to the same process in polycrystalline bulk material. In a bulk polycrystalline material, the rotation of one grain may be restricted by neighboring grains. The grain rotation has been shown to play a crucial role in grain growth processes. Moreover, it was shown that the grain rotation may be coupled with grain boundary migration. If the growth process occurs in a liquid medium *via* a particle-by-particle mode, freely standing nanoparticles could easily arrange themselves into the form of elongated single crystals. For example, nanocrystal growth based on grain rotation among neighboring grains was frequently observed in the case of colloidal nanocrystal systems such as PbSe (Fig. 2a),[31] SnO_2,[32] CdSe[33] and ZnS.[34] In all cases the process was reported to result in a coherent grain–grain interface by eliminating common boundaries, so that neighboring grains coalesce and thereby form larger nanocrystals. Recently, Moore *et al.*[35] designed a two-dimensional colloidal system to directly observe the process of grain rotation-induced grain coalescence during heating as shown in Fig. 2b.

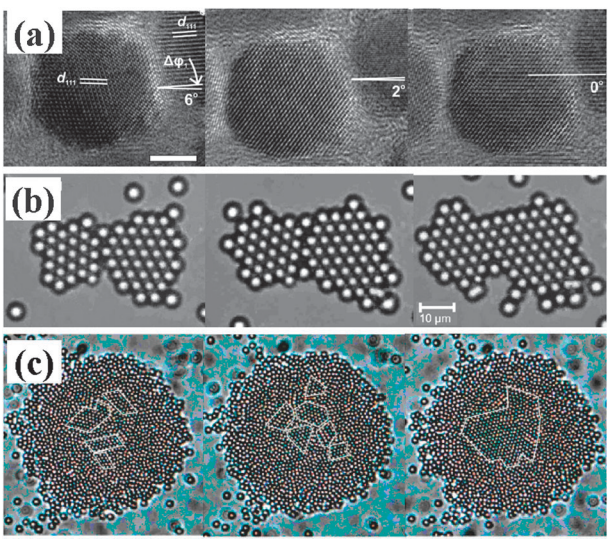

Fig. 2 (a) Representation of the mechanism *via* a grain rotation induced grain coalescence. Arrows in the second block illustrate the rotation between grains. Ref. 31, copyright American Chemical Society. Adapted with permission. (b) A typical annealing process, showing the two grains with different orientations merging to form a gain boundary, before rotation to form a crystal with a single orientation. Ref. 35, copyright American Chemical Society. Reproduced with permission. (c) Evolution of the crystalline structure inside the amorphous phase assembly of polystyrene spheres. Reprinted with permission from ref. 36. Copyright 2007, American Chemical Society.

The average time required for the annealing process was found to be in good agreement with theoretical predictions. Except for grain-rotation-induced formation of single crystals, a crystallization process of the amorphous phase may also occur. For instance, sea urchin spine calcite forms *via* a crystallization process of amorphous calcium carbonate phase[36] (Fig. 2c). Similarly, Ag crystals formed by the crystallization of amorphous matrix were found to rotate, realign and finally form a single crystalline nanostructure.[37]

Several different interpretations have been suggested to explain the driving force for the nanoparticle rotation. For example, in the case of the highly dispersed nanocrystals, the realignment of different nanoparticles was found to occur by collision processes.[32] These processes were observed in liquid as well as in gaseous environments. In fact, two kinds of collisions were found to play a role: collisions between crystals with different or the same crystallographic orientations. In the former case, coalescence does not occur and the process seems purely elastic. In the latter, a new single crystal is resulted. On the other hand, the realignment of particles in contact can be much more effective than oriented collision-induced attachments.[38] In this situation, the grain rotation induced grain coalescence is directly related to the reduction of interfacial energy. The energy reduction upon particle alignment was calculated and experimentally confirmed.[39] In fact, the energy of grain boundaries is well established to increase rapidly with increasing angle of misorientation in the range of 0–15°. Boundaries with an angular mismatch of more than 15° have practically the same energy as randomly oriented polycrystals. These results are in good agreement with the experimental results reported by H. Gleiter's group, as shown in Fig. 1.[23,24] Additionally, imperfect oriented attachment coupled with interparticle forces, *e.g.*, electrostatic interactions or polarization forces, can also result in the small angle grain rotation.[31,33]

2.2.3 Artificial syntheses of nanocrystals *via* OA mechanism. Since Lee and Banfield presented this new crystal growth mechanism, termed as "oriented attachment", this process has been utilized in several studies to synthesize nanocrystalline materials. Fig. 3 summarizes the formation of nanowires, nanorods and nanoplates through 0D1D, 0D2D, 1D1D or 1D2D self-assembly steps. Complex 3D architectures have also been explored by this self-assembly mechanisms through various assembly routes, for instance, hollow octahedra through 0D2D3D, 'dandelion'-like spheres through 1D2D3D as well as ellipsoidal nanoparticles through 0D3D methods.[15,40] However, most of the earlier reports of the synthesized nanocrystals *via* the OA process were performed by an empirical approach in the sense that materials were synthesized first and subsequently the OA mechanisms were suggested. Therefore, an intentional design to artificially synthesize nanocrystals *via* the OA process is quite rare.

It should be pointed out, however, that examples of the other approach exist as well. Huang *et al.* employed mercaptoethanol or NaOH as a strong adsorbent to ZnS nanocrystals and hindered the OR growth process, and thus finally obtained the nanocrystals *via* OA-dominated growth, containing a large number of internal lattice defects.[41] Recently, using

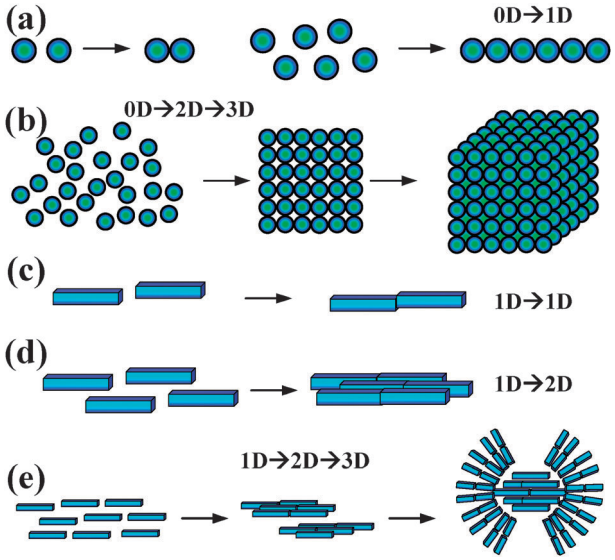

Fig. 3 Various organizing schemes for self-construction of nanostructures by oriented attachment mechanism.

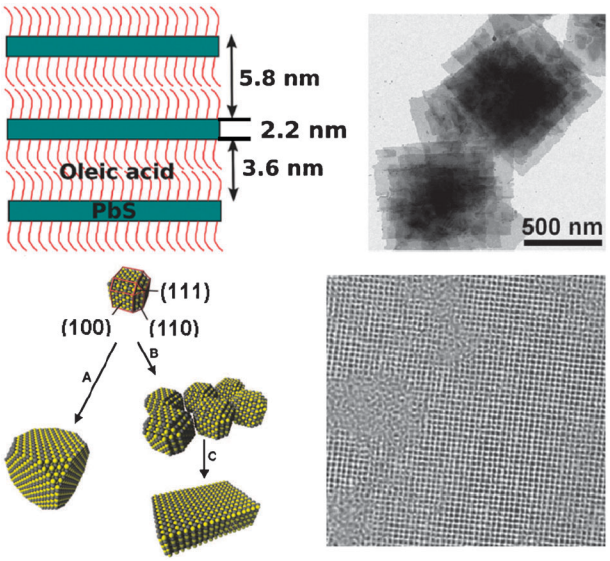

Fig. 4 Schematic formation of large-particle PdS nanosheets ref. 43, copyright 2010, sciencemag.org. Reproduced with permission.

different concentrations of surface-capped CdS quantum dots (QDs) as a precursor, they created the OA or OR dominated growth processes. Although the factors that determine the appearance of the OA or OR growth mechanism are complicated and not simply attributed to the initial concentration of QDs, they suggested that, in the high-concentration system, the density of the surfactant on CdS QDs was high, thus the OA process was more favored than the OR.[42]

The application of agents attaching to the free surfaces seems to be an effective approach to achieve the artificial syntheses of 2D OA nanostructures. Recently, Schliehe *et al.* synthesized ultrathin PbS nanosheets by a 2D oriented attachment mechanism. The selectively dense packing of oleic acid ligands on {100} facets of PbS resulted in the oriented aggregation of 2D network of PbS nanoparticles and finally the ultrathin nanosheets *via* the particle–particle fusion process.[43] The schematic illustration of the formation of large nanosheets and the corresponding TEM images of ultrasmall PbS nanosheets are indicated in Fig. 4. Huang *et al.* synthesized freestanding hexagonal Pd nanosheets that were less than ten atomic layers in thickness by a CO-confined growth method.[44] The use of CO is critical for the growth of ultrathin palladium nanosheets. Without CO, the products contain only twinned nanoparticles. Although the importance of surfactants such as poly(vinylpyrrolidone) (PVP) in producing Pd nanosheets has been suggested in previous literature, researchers believe that the strong adsorption of CO molecules on the basal (111) planes of Pd nanosheets prevents the growth along the [111] direction and directs the formation of the sheet-like nanostructures.

2.3 Nanoparticle superlattice

Before introducing the concept of mesocrystals and mesosuperstructures, we would like to briefly describe another single crystal-like superstructure—the nanoparticle (NP) superlattice, which exhibits similar structural characteristics to mesocrystals. The crystallization of matter on any length scale, from atoms and ions to biomolecules to nano- and microparticles, is of great interest for the development of new materials with potential applications in many areas such as optoelectronics, high-density data storage, catalysis, molecular electronic architectures, and biological sensing.[45] To date, methods for the crystallization of 2D and 3D NP superlattices have been explored utilizing the differences in sizes of component particles and the interparticle interactions *via* attractive forces such as van der Waals forces, the entropic effect, electrostatic forces, steric repulsion, polarization forces, hard-sphere interactions, Debye screening, small-molecule or polymer capping, hydrogen bonding, and even DNA linking strategies.[45] However, a major challenge still remains: the inability to prepare NP superlattices with well-defined sizes and shapes.[46] This is mainly attributed to the fact that the intricate fundamentals of the attractive interactions between nanoparticles in a crystal are still not understood in depth.

Along these lines the following achievements should be noted. Kalsin *et al.* investigated self-assembly of charged, equally sized metal nanoparticles of two types (gold and silver) and obtained large, diamond-like crystals with various morphologies—including octahedral, truncated tetrahedral, truncated and twinned octahedral, and triangular, which are identical to those observed for their macroscopic diamond or sphalerite (ZnS) counterparts (Fig. 5).[47] It was found that the formation of these non-closed-packed structures was a consequence of electrostatic effects specified to the nanoscale, where the thickness of the screening layer was commensurate with the dimensions of the assembling objects. By utilizing the electrostatic stabilization of larger particles aggregated by smaller ones, better-quality crystals can be obtained from more polydisperse nanoparticle solutions. Similarly, other shapes of NP superlattices have also been obtained in different materials such as Au triangles[48] and AuAg core-shells.[49]

According to the observations reported so far, the atom-mediated and nanoparticle-mediated assembly seems to be

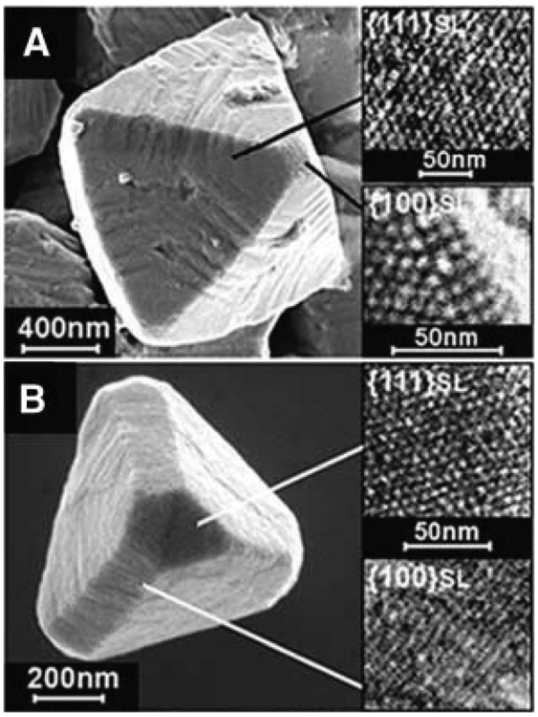

Fig. 5 Different morphologies of the AuMUA-AgTMA crystals. Ref. 47 copyright 2006, sciencemag.org. Reproduced with permission.

based on similar physical principles. This argument is further supported by a recent study reported by Rupich *et al.*[50] Twinning in atomic-mediated clusters and crystals has been a subject of intense study during the past few decades. In Rupich's work, NP superlattices aggregated by small (<4 nm) PbS nanocrystals exhibited no twins. On the other hand, owing to the twinning energy in a nanocrystal superlattice the twin density is strongly size-dependent. In fact, superlattices of large (>7 nm) PbS nanocrystals form multiply twinned face-centered cubic structures with decahedral and icosahedral symmetry, exhibiting crystallographically forbidden five-fold symmetry elements.

2.4 Mesocrystal and mesotransformation

Mesocrystals represent a separate group of colloidal crystals formed *via* the particle-mediated non-classical crystallization pathway, the so-called mesoscale transformation process. Despite the numerous studies carried out so far, there are currently still many open questions. For example, what is the actual internal structure of various materials? Different systems possess different driving forces that result in different final structures: single crystals, mesocrystals or polycrystals. On the other hand, a strong driving force can also accelerate the crystallographic fusion of the oriented nanocrystalline building units and promote the transition from mesocrystals to single crystals. Recently, a comprehensive review article was presented by Song *et al.*,[51] in which the "mesocrystals" were defined as 3D ordered nanoparticle superstructures. In fact, mesocrystals should not be only restricted into 3D structures. The 2D or 1D mesostructures with single crystallographic characteristics may equally well be summarized as 2D or 1D mesocrystals. Although several reasons explaining the mutual alignment of nanoparticles to a mesocrystal have been reported,[51] the formation mechanisms of 3D mesocrystals are largely unexplored. Hence, 2D or 1D mesocrystals may be useful model systems to understand the 3D ordered alignment processes. In addition, similar to the artificial syntheses of nanocrystals *via* the OA mechanism, artificial syntheses of mesocrystals with controllable dimensions and well-defined shapes or morphologies are still very difficult on the basis of our current existing knowledge. Therefore, a systematic strategy to investigate the growth mechanism, artificially synthetic conditions and novel properties of mesocrystals needs to be proposed in the future efforts.

2.4.1 Structural characteristics of mesocrystals. Mesocrystals usually demonstrate some intrinsic features such as rough surface, high internal porosity, small size of building block, single crystalline structure, high densities of crystalline defects and complex morphologies. However, these characteristics may vary depending on the chemical composition of materials and reaction environments. In this regard, it seems to open the way to numerous opportunities for tailoring the structures and hence all structure-dependent properties of mesocrystals.

Nanoparticles, as the building units, can also aggregate into mesocrystals with different shapes such as spheres, plates, wires or hierarchical morphologies, even within the same materials. For example, well-defined hexagonal twinned plate-like ZnO mesocrystal is built by the stacking of nanoplates.[52] The irregularly edged nanoplates can adjust themselves to each other throughout the microcrystal, resulting in a roughly hexagonal edge. From TEM and HRTEM images of the hexagonal ZnO mesocrystal, three levels of hierarchies have been deduced: nanoparticles with particle size around 20 nm, nanoplates consisting of nanoparticles and hexagonal "single crystals" formed by the stacking of well-aligned nanoplates. One can find that the self-assembly process results in microvoids. In fact, during the nanoparticle mediated transformation process, some structural features such as the size of building block, internal porosity and defects may be different even if the primary nanoparticles are initially not connected. Crystallographic fusion of nanoparticles rather than a dissolution–recrystallization mechanism is suggested to be responsible for the final porous nature of the single crystalline domains, which would not occur upon redissolution-reprecipitation in the absence of a porogen.

Although the structures of mesocrystals have been characterized in recent years by different approaches for various reaction systems, it is still an open question to understand how reaction environments influence the structures of mesocrystals and how the structural features vary during the coarsening process. In the future, this could be a critical work because these structural parameters determine the practical applications of mesocrystals.

2.4.2 Meso-intermediates transformation from mesocrystals to single crystals. The existing results imply that a mesocrystal is more a kinetic, metastable intermediate than a thermodynamically stable product. This may be one of the reasons why mesocrystals were only discovered rather recently although

examples of mesocrystals had already been reported in the literature decades ago.[7] Mesocrystals can be stable only in the case where additives or capping agents are used in the reaction system. Therefore, it is an analytical challenge to detect mesocrystals if the nanoparticle building units are not stabilized hence the crystallographic fusion of the nanoparticle subunits may occur easily. To investigate the transformation of mesocrystal to single crystal it seems promising to introduce some stabilizing molecules or to minimize the driving force of the reaction.

Recently, we demonstrate the transformation process of dendritic Ag nanostructures from mesocrystal into single crystal using a $Sn/AgNO_3$ galvanic replacement reaction.[30] By means of monitoring the structures of Ag nanostructures at different reaction time direct evidence of the conversion of mesocrystals to single crystals was obtained. This process represents an important proof for the nonclassical crystallization pathway for single crystals *via* mesocrystal intermediates. Therefore, it seems likely that many more single crystal systems are formed *via* a mesocrystal intermediate. The other experiment which is worth mentioning is the investigation of the formation of D-, L-alanine mesocrystals and their transformation into a single crystal, as was reported by Schwahn *et al.*[53] Using the time-resolved small angle neutron scattering (SANS) and dynamic light scattering (DLS), the early nanoparticle growth and the initial aggregation process to a mesocrystal were characterized. As time went on, the mesocrystal structure became compact, showing the power law scattering that gradually changed from Q^{-3} scattering (Q is the scattering vector) which represents the aggregates with an inner surface to Q^{-4} behavior characteristic for porous and compact particles.

2.4.3 Driving force of mesoassembly. It is widely known that structures and morphologies of crystals depend on the correlation between the driving force of crystallization and diffusion of atoms, ions, molecules, and/or the flow of heat. Variation in these experimental parameters can change the crystal shapes from polyhedral shapes into various complex morphologies through skeletal shapes, as well as change the crystal structures from single crystal, mesocrystal to polycrystalline. Oaki *et al.* summarized the morphological and structural evolution as a function of driving force such as the degree of supersaturation of the solutes.[54] It has been noted that a structural transition from single crystals to polycrystals may be obtained by increasing the supersaturation. Recently, Kulak *et al.*[55] carried out an experiment to study the structural evolution of calcium carbonate particles under a copolymer-mediated crystallization. Due to the strong dependence of structure and morphology on the calcium concentration, a series of calcium-ion concentrations was performed. At a fixed [Ca] : [S] molar ratio of 1.25 : 1, varying the Ca concentration can lead to a continuous transition from textured polycrystalline aggregates to mesocrystals to single crystal structures. This result is consistent with the one reported by Oaki *et al.*[54]

Growth of colloidal particles in solution is generally considered to occur either by coarsening of primary particles *via* classical ion-by-ion growth to produce single crystals or *via* nonclassical particle-mediated aggregation processes.[55] Particle-mediated aggregation can in turn produce amorphous, polycrystalline, mesostructural or single crystals, depending on the structure of the primary particles and whether the aggregation process is random or directional and whether recrystallization occurs after aggregation. Polycrystalline particles are formed preferably at high supersaturations, where rapid nucleation generates a large number of precursor nanoparticles which subsequently tend to aggregate randomly at high nanoparticle concentrations. The reduction of the supersaturation to a level where primary nanoparticles are still formed in solution yields mesocrystals. Single crystals form at low supersaturations. Here, the primary units in solution are small clusters, molecules and ions. Growth can then occur by oriented aggregation of these clusters or classical ion-by-ion addition to nascent nuclei, resulting in the formation of single crystals.

However, the reaction pathways described so far with respect to the influence of driving force on crystal structure are not the only ones. Recently, using an organic-free replacement reaction system, *i.e.*, $Sn/AgNO_3$, the influence of silver ion concentrations on the morphologies and structures of Ag nanocrystals was systematically investigated.[56] It was found that a continuous structural transition from single crystal to mesocrystals and to polycrystalline aggregates can be achieved by simply reducing the driving force of the replacement reaction, *i.e.*, silver ion concentration. Using the theory of the diffusion-controlled crystal growth, the morphological evolution under various silver ion concentrations was explained by considering the relative chemical potentials between nanocrystals and the bulk solution. Similarly, the structural transition can also be interpreted *via* the total energy of reaction system. Again in this system, the chemical potential of bulk solution was found to be the driving force for grains rotation and the realignment between small grains attached to larger crystals that had been formed before. Under growth conditions far away from equilibrium, *e.g.*, at an extremely high silver ion concentration (2 M) (Fig. 6a), the interface fusion process *via* such mutually aligned nanocrystals was found to occur readily. Therefore, the product always showed a smooth surface and in HRTEM no obvious boundaries were observed. When the silver ion concentration was reduced to a level, *e.g.*, 1 M and 200 mM (Fig. 6b), silver nanostructures were found to assemble from nanoparticles. Selected-area electron diffraction (SAED) pattern displayed a diffraction of single crystals, indicating that small grains were orderly

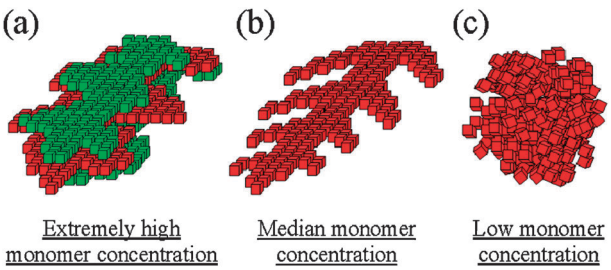

Fig. 6 Schematic illustration of monomer-concentration-dependent growth paths of Ag nanostructures synthesized from a $Sn/AgNO_3$ galvanic reaction. Single crystals, mesocrystals and polycrsytals can be formed as decreasing the monoer concentration. Ref. 56, copyright American Chemical Society. Reproduced with permission.

attached or aligned. If the chemical potential of the bulk solution was not sufficiently high to support the fusion process, mesocrystals were obtained. These arguments were further supported by the results of studies at low silver ion concentration, *e.g.*, <50 mM. Under these near equilibrium conditions, the low driving force could not support the processes such as oriented attachment, grains rotation, realignment and fusion between nanocrystals. Therefore, the product had a polycrystalline structure (Fig. 6c).

Obviously, the investigations reported so far on the influence of the driving force of a chemical reaction on crystal structure are not free of contradictions. One reason may be that different reaction environments can strongly modify the aggregation-based growth processes. Aggregation-based mechanisms can lead to the formation of highly ordered particle assemblies and also the non-oriented polycrystalline particles. However, we are still far away from a full understanding with respect to the foundational rules to tailor the particle aggregation as desired way.

2.4.4 Mechanisms of ordered mesoarchitecture. In recent years, although more and more mesocrystals have been reported from various experiments, the understanding of underlying growth mechanisms of ordered aggregation remains very poor. An impressive review paper was reported by Cölfen's group.[51] In this paper, Song *et al.* proposed four principal possibilities to explain the 3D mutual alignment of nanoparticles to a mesocrystal including (a) alignment of nanoparticles by an oriented organic matrix, (b) nanoparticle alignment by physical fields or mutual alignment of identical crystal faces, (c) epitaxial growth of a nanoparticle employing a miner bridge connecting the two particles and (d) nanoparticle alignment by spatial constraints.

According to available arguments, including recent experimental findings and our results, it seems that a common crystallization framework can be figured out to describe the formation of mesocrystals, which is displayed in Fig. 7. The proposed model of ordering architecture of mesostructures is related to both the intrinsic crystal structure and external growth environment. In the proposal from Cölfen's group, four principle possibilities of ordered aggregation were considered to be controlled by the external environments such as the organic matrix or polymer adsorption, applied physical fields, and so on. However, in fact, research implied that the thermodynamically intrinsic feature of a crystal such as the surface energy and the shape or size of nanoparticle building blocks may play a more prominent role.

Mesocrystal or ordered *meso*-assembly was developed on the basis of the observation of the OA and of grain rotation processes. The OA mechanism, the spontaneous self-organization of adjacent particles, can be driven by reducing the overall energy due to removing surface energy associated with unsatisfied bonds. There is a strong thermodynamic driving force for OA process because the surface energy is reduced substantially when the interface is eliminated. This may also occur when particles nucleate side-by-side on a substrate and coalesce during growth. In a solution reaction, various shapes of clusters or nuclei (Fig. 7) can be formed depending on the reaction conditions. These diverse shapes and sizes of nanoparticle subunits provide many

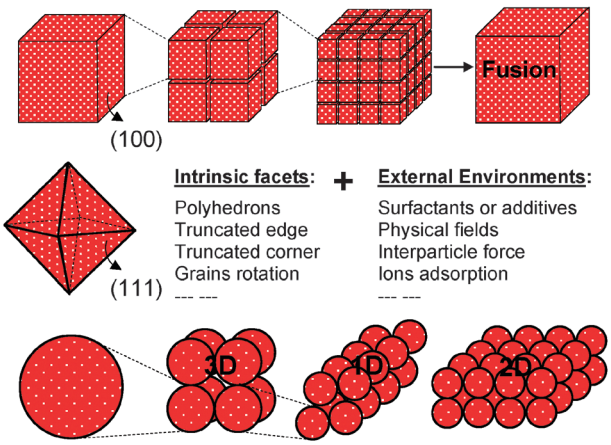

Fig. 7 The proposed common crystallization framework according to contributions from intrinsic crystal structure and external growth environment.

ways for the further orderly anisotropic aggregation if a non-classical crystallization route applies. For a face centered cubic (fcc) crystal structure, the surface energies of the low-index crystallographic facets is given in the order $\gamma\{111\} < \gamma\{100\} < \gamma\{110\}$.[3] As a consequence, the Gibbs–Wulff shape for an fcc crystal structure is a truncated octahedron. Although truncation introduces a relatively high-energy {100} facet, it generates nearly spherical shape, thereby decreasing the total surface area and free energy. As a spherical single-crystalline particle, its surface must contain high-index crystallography planes, thus it results in an enhanced surface energy.[57] Therefore, if a particle-mediated crystallization occurs, not only polyhedrons prefer to assemble into the anisotropic morphology, but spherical nanoparticles may also anisotropically grow along a preferred directions to remove the high-index crystallography planes as shown in Fig. 7. In fact, mesocrystals consisted of polyhedral or spherical building units have been reported from recent investigations.[15,16,58]

Following the oriented aggregation process, the grain rotation can also further optimize the crystallography ordering. Small nanoparticle building units possess much higher surface energy than micrometre-sized particles or even bulk materials with the same chemical compositions. Thus, in nanometre scale, the grain rotation may also further eliminate the misorientation energy hence form mesocrystals or single crystals.

Why can mesocrystals always show a well faceted appearance? In classical crystallization, the shape of crystals grown in solution is thermodynamically defined by minimizing the interfacial energies and the area of the free surfaces (Wulff's rule). This rule likely undergoes a generalization when nanocrystalline assemblies or mesocrystals are involved, including the formation of minimal surfaces in the intermediates of the pseudo-dodecahedral and curved faces in the pseudo-octahedral crystals. Mesocrystals with well-defined faceted morphology have been reported in many materials.[8,9,11–14,40] Most likely, in addition to the thermodynamically driven intrinsic crystal structure, the interparticle forces also play a substantial role during the formation of mesoscale assemblies.

Additionally, internal voids, as a common structural feature that has been observed in most of mesocrystals, may also affect ordering of the aggregation and the realignment

processes. In the vicinity of internal voids, more free atoms exist, which provide space for the further rearrangement of misaligned nanometre-sized building units. The high density of defects observed in the vicinity of internal voids seems to support this argument.

In addition to the intrinsic crystal structure of the building block, the growth conditions may play an important role as well in determining the ordered mesoscale assembly. The external factors discussed above, such as oriented organic matrix, physical fields, polymer adsorption as well as spatial constraints may affect the ability of mesocrystals to form. Polymers may slow down the transition from mesocrystals to single crystals. Externally applied fields may promote the ordering alignment for initially mis-oriented crystals. On the other hand, these external factors could modify the intrinsic growth behavior of a crystal. For example, with the assistance of surfactants that are adsorbed preferentially on specific planes of inorganic crystals, the oriented-attachment mechanism seems to be an efficient way of producing anisotropic structures. Therefore, mesocrystals could be generated in systems consisting initially of single crystals or polycrystals. However, so far, the formation processes of mesocrystals are still poorly understood. This applies in particular to 3D mesocrystals. Theoretical models of these processes have not yet been developed due to the lack of the experimental basis.

2.4.5 Artificial synthesis of mesocrystals. Similar to the situation of the artificial synthesis of materials *via* the OA mechanism, most reports on mesocrystals are still purely descriptive. Predictions of what kind of mesocrystals will form for a given system and experimental parameters are not yet possible. Therefore, reports on the controlled syntheses of mesocrystals are still missing.

Recently, an external electric field driven particle-mediated "bottom-up" assembling of Ag_2O mesocrystals has been reported with controlled shape and size within an electrochemical deposition system (see Fig. 8).[8] Different shapes (rhombic hexahedron, cube and dodecahedron) and sizes (around 100–800 nm) of Ag_2O mesocrystals have been obtained by varying the applied overpotential and the growth time. An unusual high overpotential plays a crucial role in determining the shapes, structures and growth modes of the final product. In fact, the applied electric field induced ordered alignment of primary nanocrystals and the oriented attachment. The crystallographic orientation of the facets was suggested to explain the formation of the Ag_2O mesocrystals resulting in various polyhedral shapes. These experiments provide direct evidence for the possibility to artificially synthesize mesocrystals by means of an external electric field. This approach may likely be extended to other systems.

In fact, existing investigations indicated that ordering mesoassembly of particles with "mesocrystal structures" are likely to occur if (1) the supersaturation is sufficiently high for the crystallization pathway to be controlled kinetically.[55] Previous studies of the synthesis of Ag mesocrystals[56] as well as crystal growth in gels[8] have indicated that high supersaturations and high particle nucleation rates (forming abundant small clusters—the building blocks for the mesocrystals) induce preferentially mesocrystal formation rather than the ion mediated classical crystallization process. (2) Intrinsic and/or externally applied fields enhance the ordering aggregation. (3) The nucleation processes are well controlled, the primary nanoparticle subunits display well defined shapes. In the near future, further mechanisms and rules are likely to be exploited to artificially synthesize mesocrystals.

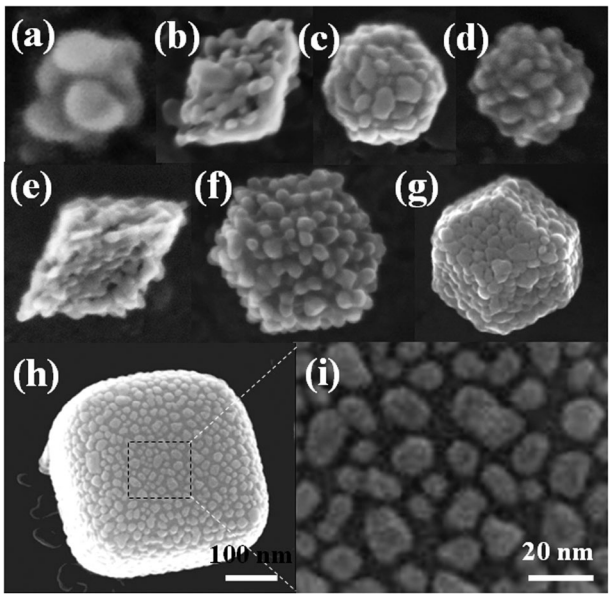

Fig. 8 FESEM images of Ag_2O mesocrystals synthesized by electrodeposition. (a) aggregate of Ag_2O nanoparticles (b)–(d) typical quasi-polyhedral Ag_2O mesostructures with approx. 50 nm in size. (e)–(g) polyhedral Ag_2O mesocrystals with around 100 nm in size. (h) A typical Ag_2O mesocube with about 500 nm in size. (i) The high magnification image taken from the boxed area in Fig. 8h. Ref. 8, copyright 2010, reproduced with permission from Elsevier.

3. Mesocrystals in metals

In recent years, more and more mesocrystals have been reported. However, most of the studies on mesocrystals focus on biomimetic materials (*e.g.* Calcium carbonate, Mg-calcite), metal oxides (*e.g.* Ag_2O,[8] Cu_2O,[9] ZnO,[10] TiO_2),[11] sulfide (*e.g.* CdS, PdS), or other inorganic materials (*e.g.* CeF_3, ZnSe, $AgInWO_4$,[12,13] PdSe).[16] Very few studies on metal mesocrystals have been published up to now. In fact, metal mesocrystals or mesostructures generated by a controlled bottom-up assembly process into superstructures will create new optical or catalytic properties due to mutual interactions of the nanoparticles building units. Therefore, in this short section, we summarize the recent work on the syntheses of metal mesocrystals.

3.1 Au dendrites

A report from our previous experiment demonstrated the early evidence on the mesocrystal in metals. Gold dendritic mesostructures were synthesized in aqueous solutions by means of a simple and fast electroless metal deposition route from $Zn/HAuCl_4$ (aq).[17] HRTEM investigations revealed that the gold dendrites have a threefold symmetry. The dendrites consisted of numerous nanocrystals with a size of 5–10 nm. Moreover, the aggregated nanoparticles spontaneously self-assemble along

⟨211⟩ crystallographic orientations and form a single crystalline dendrite. From the HRTEM image, the nanoparticle building units display a spherical shape. Thus, it seems that the intrinsic crystal structure of the subunits provides an important contribution to the anisotropic growth along ⟨211⟩ orientations, *i.e.*, a high-index crystallographic planes. The oriented attachment mechanism was suggested to account for the nanoparticle-aggregated self-assembly process. The novel gold dendritic nanostructure may be useful for surface-enhanced Raman scattering (SERS) and other applications.

3.2 Ag mesoplates

By using a straightforward organic-free replacement reaction system, Sn/$AgNO_3$ (aq.), 2D single crystalline silver mesocrystals with a size of about 5–20 μm and a thickness of 70 nm were synthesized.[18] TEM images and the corresponding SAED patterns recorded from at least four-layer silver plates revealed that the four-layer silver plate is a single crystal. Nucleation was noted to occur preferentially at uniformly spaced dislocation sites or the deformation areas of the reconstructed surface layer. After nucleation, a subsequent OA dominated the self-assembling process of single-crystalline silver plates involving attachment, rotation, and re-alignment of the nanometre-sized crystals.

3.3 Au mesoflowers

Particle mediated aggregation of "sea urchin"-like gold mesoparticles with tailored surface topography was utilized to synthesize Au mesostructures.[59] The general method used to synthesize the Au sea urchin-like mesoparticles is based on a secondary nucleation and growth process as shown in Fig. 9a. During the growth of Au nanocrystals, an atomic concentration fluctuation in the reaction solution is created by quickly injecting a certain amount of Fe suspension again. This injection induces a secondary nucleation and growth process. By varying the conditions of this process, the surface texture of the mesoparticles may be systematically tailored. "Meatball" morphology, II and IV, is formed if moderate amounts of Fe are injected. Furthermore, the surface texture may be changed from type II to type IV by delaying the second injection, *e.g.*, from 5 to 10 min after the start of the reaction (Fig. 9b). If a larger amount of Fe is injected, it changes the product morphology to strongly textured types III (ower-like) and V (sea urchin-like) structures.

The number and density of the spikes on the particles of type V can be additionally enhanced by increasing the amount of Fe in the second injection. The current results seem to indicate that a mesoscale transformation process occurs preferably either at high supersaturations or at high particle nucleation rate (*e.g.*, a relatively high concentration of $HAuCl_4$). In this situation, abundant small clusters, *i.e.*, the building blocks for the mesostructures, induce mesocrystal formation rather than the atom-mediated classical crystallization. At low reduction and nucleation rates, Au particles are likely grow near thermodynamic equilibrium *i.e. via* the "classical" atom-by-atom growth process.

3.4 Ag nanocolumns

Qi and colleagues synthesized hierarchical Ag nanocolumns by means of a polymer-controlled crystallization process when

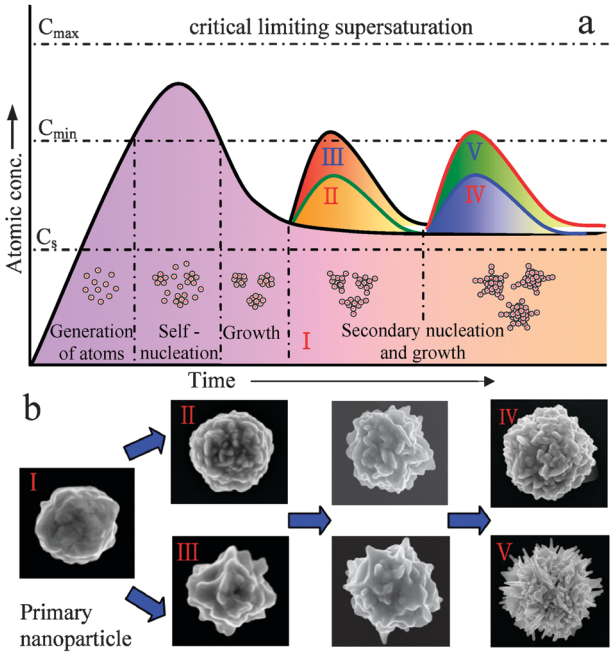

Fig. 9 Schematic plot of (a) gold atom concentration *versus* time illustrating the growth of mesoparticles, including the generation of atoms, nucleation, subsequent growth, secondary nucleation and mesoscopic aggregation. (b), SEM images of a variety of surface topographies, types *I–V*, synthesized at various conditions. Ref. 59 copyright 2010, American Chemical Society. Reproduced with permission.

acetic acid (HAc) was introduced into the reaction solution consisting of poly (acrylic acid) (PAA) and $AgNO_3$.[60] The hierarchical silver nanocolumns consisted of stacked nanoplates with diameters of typically 300–500 nm. The high-magnification SEM image suggested that the nanocolumns were composed of face-to-face stacked nanoplates with a thickness about 20–40 nm. The diffraction pattern indicated that the nanocolumn was a single crystal grown along the [111] direction and all the face-to-face stacked nanoplates were [111]-oriented. This morphology may be understood by assuming that the silver nanocolumns were formed by step-by-step growth process of nanoplates at the top surface of pre-formed nanoplates or nanocolumns, *i.e.*, the stacks developed by gradual propagation of surface steps from a primary [111]-oriented single-crystalline nanoplate.

This example indicates the interaction of surfactants with the intrinsic growth of crystals along specific crystallographic facets. A cooperative effect from PAA and HAc contributes to the formation of Ag nanocolumns. The central part of the growth front adsorbs fewer capping ions during the growth process hence grows fastest. This high growth rate leads to the nucleation of another nanoplate from the central part of the top surface of the primary nanoplate. Finally silver nanocolumns made by stacked nanoplates are formed.

3.5 Pt, PtRu mesopolyhedrons

Other interesting examples of metal mesocrystals were reported recently during the syntheses of Pt and PtRu mesopolyhedrions.[61–63] Lim *et al.* synthesized highly faceted Pt nanocrystals with a large number of interconnected arms

in a quasi-octahedral shape (Fig. 10a). The synthesis was performed by reducing H_2PtCl_6 precursor with poly (vinyl pyrrolidone) in aqueous solutions containing a trace amount of $FeCl_3$.[61] The iron species (Fe^{3+} or Fe^{2+}) play a key role in inducing the formation of the multioctahedral structure by decreasing the concentration of Pt atoms and keeping a low concentration for the Pt seeds during the reaction. This condition favors the overgrowth of Pt seeds along their corners and thus the formation of multi-armed nanocrystals. HRTEM image and the corresponding Fourier transform (FT) pattern (Fig. 10b and its inset) indicate that the multi-octahedral Pt nanocrystal was one portion of a single crystal. The evolution of multi-octahedral morphology could be attributed to overgrowth of initially formed octahedral Pt seeds at their corner sites. In fact, the overgrowth of Pt nanocrystals has been observed at low concentrations of seeds and high concentrations of Pt atoms. Teng *et al.* presented a different approach to the synthesis of PtRu nanostructures with defined shapes (see Fig. 10c).[62] The selected capping of different low indexed surfaces by adamantaneacetic acid and hexadecaneamine led to the formation of cubic or tetrahedral nanodendrites from faceted primary nanoparticles. Most likely this structure is formed by an oriented attachment process. Recently, Nogami *et al.*[63] also obtained porous single crystalline Pt nanocubes which were composed of nanoparticles with around 5 nm in size (Fig. 10d).

The above results indicate that the shape of mesocrystals depends on the initial intrinsic growth feature of the nanometre-sized building units. When the seed crystals are of polyhedral nature, the secondary growth occurs preferentially along less protected crystallographic faces, so that an anisotropic mesostructure with well-defined morphology results.

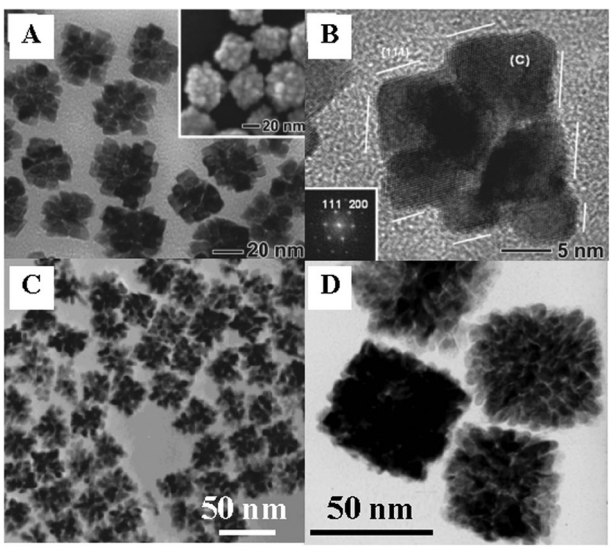

Fig. 10 (a)–(b) TEM images multioctahedral Pt nanocrystals. Ref. 61, copyright 2008, American Chemical Society. Reproduced with permission. (c) TEM image of PtRu nanodendrites. Ref. 62, copyright 2007, American Chemical Society. Reproduced with permission. (d) TEM image of Pt nanocubes. Ref. 63, copyright 2010, American Chemical Society. Reproduced with permission.

3.6 Ag mesodendrtie

In our earlier studies, a dendritic silver nanostructure was synthesized in $AgNO_3$ (aq) at ambient temperature without surfactants.[19] The non-equilibrium and anisotropic growth at different silver ion concentrations resulted in well controlled morphologies and morphological evolutions. At high silver ion concentrations, a strong anisotropic growth led to fine single crystalline silver dendrite. However, at relatively low silver ion concentrations, fractal arrangements of aggregated particles were obtained due to relatively small anisotropy. As the reaction time increased, the transition from polycrystalline aggregates to a single crystal during silver dendritic growth was observed. An oriented attachment mechanism was suggested to explain the structural and morphological evolution of silver nanostructure. The defects originated from the imperfect assembling of several small aggregates can always be observed. The presence of a series of edge dislocations at self-assembling interfaces is in good agreement with earlier studies of "oriented attachment" in other systems as was reported by Banfield *et al.*[5] Silver mesodendrites with various morphologies may have applications to generate superhydrophobic surface and surface-enhanced Raman scattering (SERS).

Additionally, oriented attachment as a growth mechanism has also been reported for other noble metals in the form of "flowerlike" Ag nanoplates[64] as well as Pt nanodendrites.[65]

4. Novel properties of mesocrystals

The use of nanoparticles as building blocks for the bottom-up fabrication of superstructures has been shown to be an important approach to obtain novel materials with collective properties. Nanocrystals with different chemical and physical properties are readily available and combining these nanoparticles and mixtures thereof gives access to an almost indefinite number of possibilities to tailor the properties of a material. As mentioned above, owing to the unique structure of mesocrystals such as rough surface, high internal porosity, small size of building block, single crystalline structure, high crystalline defects as well as complex morphology, they are ideally suited to many applications like catalysts, sensors, and optical devices. Although the relative investigations with regard to the correlations between structures and properties of mesocrystals are still quite few, the available reports have showed that this unique structure of mesocrystals makes them very attractive for very wide potential applications. Thus, in section 4 of this review, we summarize some of the latest results regarding the properties of mesocrystals. However, we discuss them in a variety of materials, not only in metals but also in oxides or compounds.

4.1 SPR and SERS

In Fig. 9, mediated aggregation utilized to synthesize "sea urchin"-like gold mesoparticles with tailored surface topography is shown. Surprisingly, these multi-tip Au mesoparticles are capable of self-assembling into monolayer or multiple layer arrays on Si substrates with remarkable reproducibility and homogeneity over large areas as shown in Fig. 11a and b. Raman measurements indicate that the individual sea urchin-like and multi-tipped gold mesoparticles exhibit a high SERS

enhancement. In addition, the sea urchin-like mesoparticle arrays display a further enhancement of SERS by one or two orders of magnitude relative to the individual mesoparticle due to the formation of additional hot spots between the particles (Fig. 11c–d).

4.2 Catalyst and electrocatalyst

It was noted that the activity and stability of a metal nanostructure can be enhanced by controlling the aggregations of small nanoparticle building units. Recently, Lim,[61] Teng[62] as well as Nogami[63] *et al.* prepared Pt, PtRu mesopolyhedrons (Fig. 10) and investigated their catalyst and electrocatalytic properties. In all cases, Pt or PtRu mesostructures exhibited improved specific activity as compared to commercial Pt-based catalysts. Of course, the crystal morphology, *e.g.*, crystal orientation of surface facets affects its chemical activity. In fact, it is believed that the particle mediated aggregation process plays an important role in determining the shapes, morphologies as well as the final structures of the aggregate. Particularly, these catalysts demonstrate a high stability and durability because the crystallographically single-crystal-like mesostructures would be helpful to maintain a high surface area. This argument seems to be supported by a recent paper on the investigation of lithium ion storage of TiO_2 mesocrystals,[66] in which the anatase could be retained even after being annealed at 900 °C, owing to the interfacial nucleation sites were largely eliminated because the crystallographically oriented nanocrystals were connected by mineral necks in the single-crystal-like anatase mesocrystals, leading to a remarkably enhanced phase stability.

4.3 Sensor application

Hu *et al.* synthesized monodisperse ZnO nanocrystals by a microwave-polyol process.[10] The particle size could be tuned from 50 to 300 nm. The HRTEM image and the SAED pattern clearly revealed that small primary nanocrystals with sizes of 6–10 nm were present in these ZnO particles. In fact, every ZnO particle turned out to be one single crystal. The formation of these ZnO nanocrystals could be explained by the well known growth mechanism involving "oriented attachment".

The high sensitivity and reversibility for humidity sensing of these films seem remarkable. These properties seem to be based on the unique nanostructure of the ZnO films consisted of nanocrystallites, inter-cluster pores and large internal surfaces and a network of interconnected hierarchical pores. This microstructure differs significantly from conventional film-type sensors consisted of compact ZnO particles. The network of hierarchical inter-nanocrystallite and inter-cluster pores seem to be crucial for the high sensitivity, since it allows the water molecules to attach the large internal surfaces of ZnO colloidal nanocrystals.

The sensitivity of the thin film sensor was noted to show a pronounced size-dependence. An enhanced area of internal surfaces-attributed to the smaller crystal size—results in an increased sensitivity. This seems to apply to crystal sizes of 100 nm or larger. However, if the diameter of crystal is reduced to 86 and 57 nm, the sensitivity does not improve further but actually drops slightly. Clusters with sizes between 87–125 nm seem to possess the optimal inter-cluster porosity and internal surface area to achieve the highest performance in the case of ZnO nanocrystals for humidity sensing.

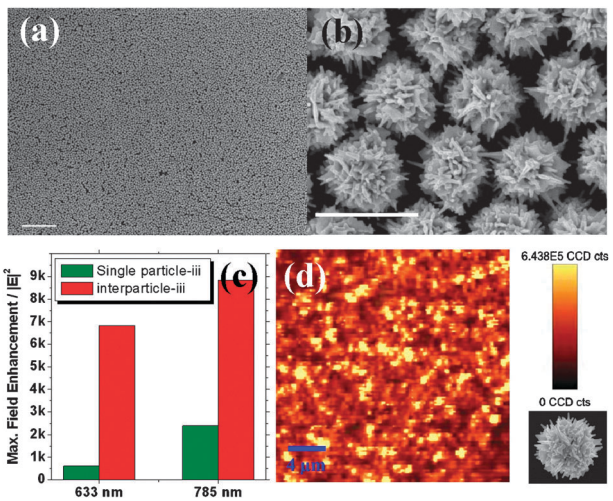

Fig. 11 (a) SEM image of a dense monolayer array of sea urchin-like mesoparticles self-assembled on a silicon wafer; (b) the magnied SEM image and (c) the maximum field enhancement for single particle and two interacting particles at various wavelengths from DDA calculations; (d) Raman images of the arrays. The scale bars shown in (a) and (b) correspond to 20 and 1 μm. Ref. 59, copyright 2010, American Chemical Society. Reproduced with permission.

4.4 Terahertz radiation

Recently, Chu's group reported novel uniform-sized, core-shell ZnO mesocrystal microspheres which were synthesized on a large scale by using a simple one-pot hydrothermal method in the presence of the water-soluble polymer poly (sodium 4-styrenesulfonate) (see image in Fig. 12a).[67] The intrinsic dipole field introduced by the nanoplatelets plays an important role throughout the mesoscale assembly process to create the apple-like core/shell bimesocrystalline structure. Very recently, they incorporated this novel mesostructure into the terahertz-emitting materials.[68] In fact, the apple-like ZnO mesocrystals used in these materials were composed of hexagonal core and the microsphere shells that were made up by a great number of hexagonal ZnO nanoplates as is shown schematically in Fig. 12b and the inset of Fig. 12a. When the material was excited by continuous green laser light, high-frequency mechanical vibrations and radiative emission at ~0.36 THz were observed. It was found that ~0.016% of incident power was converted into terahertz radiation, which corresponds to a quantum efficiency of ~33%. This high efficiency makes the ZnO microspheres competitive with the best existing terahertz-emitting materials. The origin of this terahertz vibration mode was found to be determined by the microsphere structure and its spectral characteristics.

Accordingly, the vibrations are closely associated with the high-frequency vibration of the photo-induced single hexagonal ZnO nanoplates. Subsequently these vibrations propagate due to elastic and electrical coupling between the nanoplates.

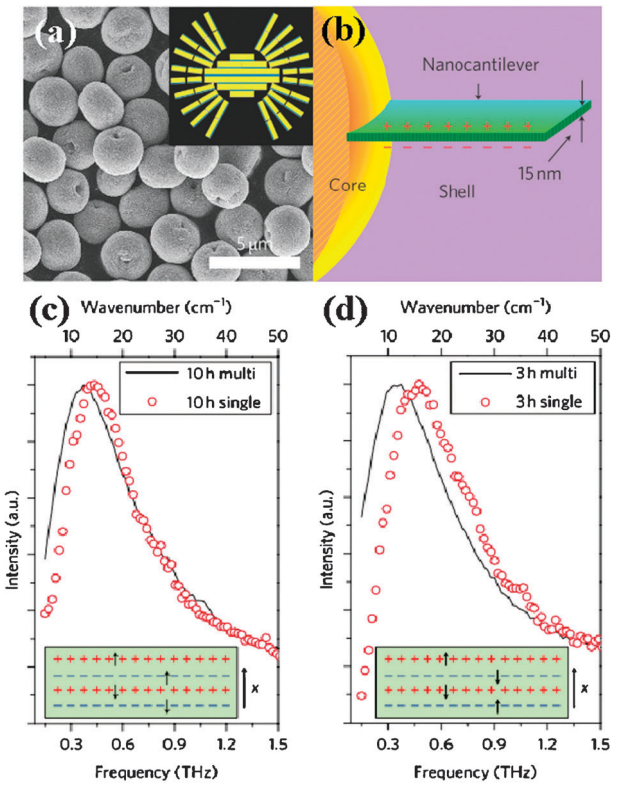

Fig. 12 (a) FE-SEM image and schematic illustration of the ZnO mesocrystal microspheres. (b) Schematic of a nanocantilever with thickness of 15 nm. (c)–(d) vibration spectra of single and multi-microsphere samples with different synthesis times. (c) 10 h, (d) 3 h. Ref. 68, copyright 2010, Macmillan publishers limited. Reproduced with permission.

Therefore, the propagation of vibration within individual microspheres or in multi-microsphere systems can be tuned by varying the shapes of the crystal. As a consequence, the frequency may be affected by changing the sizes of microspheres (relative to reaction time) and the ordering of individual nanocantilevers as shown in Fig. 12c and d. This is a simple and efficient approach for generating terahertz radiation. In fact, it may be possible to increase their efficiency further by adopting effective mirror reflection or designing hierarchical nanostructures. Their integration into nanoscale devices may allow novel applications like microscale medical imaging and microdisplacement driving.

In addition to above typical mesostructure-dependent properties, some mesostructure-related properties have also been reported recently. We would like to point out that the Ag mesoplates reported by Sun *et al.*,[64] mesoscopic Au "metaball' particle reported by Wang *et al.*,[69] the "flower-like" silver nanoparticles reported by Liang *et al.*,[70] exhibited an improved SERS property due to the rough surface feature attributed to mesoscale transformation. Zheng *et al.* also reported strong defect-induced photoluminescence characteristic for CdS quantum dots.[42] Hence, if—by means of OA growth of CdS quantum dots—a high density of defects is introduced into these materials, they are likely to have higher defect-induced luminescence than materials obtained *via* the OR route.

5. Conclusions and outlook

Because the ensembles of nanoparticles can exhibit collective properties that are different from those displayed by individual nanoparticle and bulk materials, self-assembly of nanoparticles, as a powerful technique to form ensembles, has shown its tremendous potentials to integrate nanoparticles into well-defined structure hence create novel properties of ensembles of nanoparticles. Mesocrystals resulted from the non-classical crystallization route as a unique ordering nanoparticle superstructure possess unique structural characteristics including rough surface, high internal porosity, small size of building block, single crystalline structure, high crystalline defects as well as complex morphology. Materials with such features are believed to be ideally suited to many applications such as catalysts, sensors, optical devices, and so on. However, up to now, the following fundamental aspects remain largely unexplored.

First, what is the underlying growth mechanism during the highly ordered mesoscale assembly? Recently, Song *et al.* summarized several possibilities to form a mesocrystal. However, it seems that the intrinsic crystal structure of the building block may equally play an important role in the oriented aggregation. Therefore, in this review, we figure out a common crystallization framework to attract more attentions to the investigations of the initial nucleation stage. Some approaches such as molecule dynamic simulations or *in situ* observations, *i.e.* by small angle X-ray scattering, would be effective to give insight into the formation of nanoparticle building units.

Second, how can we employ this unique growth mode to artificially synthesize advanced functional materials in a controlled way remains largely unexplored. In fact, we do not know what experimental parameters in a given reaction system are required to form a mesocrystal with well-defined morphology. Therefore, we need to continuously explore the growth rules of ordering mesoscale assembly.

Third, what novel properties may be exploited from this unique mesostructure relative to the perfect single crystal or polycrystalline structure with the same chemical composition? The existing investigations have shown obvious evidence that advanced functions can be obtained *via* mesostructures. However, it is still a challenge to extend the applications of mesocrystals because so far their formation processes and controlling rules are still poorly understood.

Acknowledgements

J. X. Fang was supported by the Tengfei Talent project of Xi'an Jiaotong University, "New Century Outstanding Talents" by the Ministry of Education of China, the Fundamental Research Funds for the Central Universities (No. 08142008), the National Basic Research Program of China (No. 2010CB635101).

References

1 Y. N. Xia, Y. J. Xiong, B. Lim and S. E. Skrabalak, *Angew. Chem., Int. Ed.*, 2009, **48**, 60.
2 H. J. You, J. X. Fang, F. Chen, M. Shi, X. P. Song and B. J. Ding, *J. Phys. Chem. C*, 2008, **112**, 16301.

3 G. Wulff, *Z. Kristallogr*, 1901, **34**, 449.
4 T. X. Wang, H. Cölfen and M. Antonietti, *J. Am. Chem. Soc.*, 2005, **127**, 3246.
5 R. Lee Penn and Jillian F. Banfield, *Science*, 1998, **281**, 969.
6 H. Kuhn, G. Baero and H. Gleiter, *Acta Metall.*, 1979, **27**, 959.
7 A. W. Xu, M. Antonietti, H. Cölfen and Y. P. Fang, *Adv. Funct. Mater.*, 2006, **16**, 903.
8 J. X. Fang, P. M. Leufke, R. Kruk, D. Wang, T. Scherer and H. Hahn, *Nanotoday*, 2010, **5**, 175.
9 X. D. Liang, L. Gao, S. W. Yang and J. Sun, *Adv. Mater.*, 2009, **21**, 2068.
10 X. L. Hu, J. M. Gong, L. Z. Zhang and J. C. Yu, *Adv. Mater.*, 2008, **20**, 4845.
11 S. J. Liu, J. Y. Gorig, B. Hu and S. H. Yu, *Cryst. Growth Des.*, 2009, **9**, 203.
12 B. Hu, L. H. Wu, Z. Zhao, M. Zhang, S. F. Chen, S. J. Liu, H. Y. Shi, Z. J. Ding and S. H. Yu, *Nano Res.*, 2010, **3**, 395.
13 B. Hu, L. H. Wu, S. J. Liu, H. B. Yao, H. Y. Shi, G. P. Li and S. H. Yu, *Chem. Commun.*, 2010, **46**, 2277.
14 X. Geng, L. Liu, J. Jiang and S. H. Yu, *Cryst. Growth Des.*, 2010, **10**, 3448.
15 A. W. Xu, M. Antonietti, S. H. Yu and H. Cölfen, *Adv. Mater.*, 2008, **20**, 1333.
16 K. S. Cho, D. V. Talapin, W. Gaschler and C. B. Murray, *J. Am. Chem. Soc.*, 2005, **127**, 7140.
17 J. X. Fang, X. N Ma, H. H. Cai, X. P. Song and B. J. Ding, *Nanotechnology*, 2006, **17**, 5841.
18 J. X. Fang, B. J. Ding and X. P. Song, *Appl. Phys. Lett.*, 2007, **91**, 083108.
19 J. X. Fang, H. J. You, P. Kong, Y. Yi, X. P. Song and B. J. Ding, *Cryst. Growth Des.*, 2007, **7**, 864.
20 M. Niederberger and H. Cölfen, *Phys. Chem. Chem. Phys.*, 2006, **8**, 3271.
21 H. Cölfen and M. Antonietti, *Angew. Chem., Int. Ed.*, 2005, **44**, 5576.
22 Q. Zhang, S. J. Liu and S. H. Yu, *J. Mater. Chem.*, 2009, **19**, 191.
23 D. G. Brandon, *Acta Metall.*, 1966, **14**, 1179.
24 G. Herrmann, H. Gleiter and G. Baro, *Acta Metall.*, 1976, **24**, 353.
25 D. Moldovan, V. Yamakov, D. Wolf and S. R. Phillpot, *Phys. Rev. Lett.*, 2002, **89**, 206101.
26 M. Yeadon, M. Ghaly, J. C. Yang, R. S. Averback and J. M. Gibson, *Appl. Phys. Lett.*, 1998, **73**, 3208.
27 R. L. Penn and J. F. Banfield, *Geochim. Cosmochim. Acta*, 1999, **63**, 1549.
28 F. Huang, H. Z. Zhang and J. F. Banfield, *Nano Lett.*, 2003, **3**, 373.
29 H. Q. Zhan, X. F. Yang, C. M. Wang, C. L. Liang and M. M. Wu, *J. Phys. Chem. B*, 2010, **114**, 14461.
30 J. X. Fang, B. J. Ding, X. P. Song and Y. Han, *Appl. Phys. Lett.*, 2008, **92**, 173120.
31 M. A. van Huis, L. T. Kunneman, K. Overgaag, Q. Xu, G. Pandraud, H. W. Zandbergen and D. Vanmaekelbergh, *Nano Lett.*, 2008, **8**, 3959.
32 C. Ribeiro, E. J. H. Lee, T. R. Giraldi, E. Longo, J. A. Varela and E. R. Leitem, *J. Phys. Chem. B*, 2004, **108**, 15612.
33 Z. H. Yu, M. A. Hahn, S. E. Maccagnano-Zacher, J. Calcine, T. D. Krauss, E. S. Alldredge and J. Silcox, *ACS Nano*, 2008, **2**, 1179.
34 H. Z. Zhang and J. F. Bandield, *Nano Lett.*, 2004, **4**, 713.
35 L. J. Moore, R. D. Dear, M. D. Summers, R. P. A. Dullens and G. A. D. Ritchie, *Nano Lett.*, 2010, **10**, 4266.
36 T. H. Zhang and X. Y. Liu, *J. Am. Chem. Soc.*, 2007, **129**, 13520.
37 J. X. Fang, H. J. You, P. Kong, B. J. Ding and X. P. Song, *Appl. Phys. Lett.*, 2008, **92**, 143111.
38 E. J. H. Lee, C. Ribeiro, E. Longo and E. R. Leite, *J. Phys. Chem. C*, 2005, **109**, 20842.
39 W. T. Read and W. Shockley, *Phys. Rev.*, 1950, **78**, 275.
40 H. G. Yang and H. C. Zeng, *Angew. Chem., Int. Ed.*, 2004, **43**, 5930.
41 J. Zhang, Z. Lin, Y. Z. Lan, G. Q. Ren, D. G. Chen, F. Huang and M. C. Hong, *J. Am. Chem. Soc.*, 2006, **128**, 12981.
42 J. S. Zheng, F. Huang, S. G. Yin, Y. J. Wang, Z. Lin, X. L. Wu and Y. B. Zhao, *J. Am. Chem. Soc.*, 2010, **132**, 9528.
43 C. Schliehe, B. H. Juarez, M. Pelletier, S. Jander, D. Greshnykh, M. Nagel, A. Meyer, S. Foerster, A. Kornowski, C. Klinke and H. Weller, *Science*, 2010, **329**, 550.
44 X. Q. Huang, S. H. Tang, X. L. Mu, Y. Dai, G. X. Chen, Z. Y. Zhou, F. X. Ruan, Z. L. Yang and N. F. Zheng, *Nat. Nanotechnol.*, 2011, **6**, 28.
45 M. R. Jones, R. J. Macfarlane, B. Lee, J. Zhang, K. L. Young, A. J. Senesi and C. A. Mirkin, *Nat. Mater.*, 2010, **9**, 913.
46 S. C. Glotzer and J. A. Anderson, *Nat. Mater.*, 2010, **9**, 885.
47 A. M. Kalsin, M. Fialkowski, M. Paszewski, S. K. Smoukov, K.J. M. Bishop and B. A. Grzybowski, *Science*, 2006, **312**, 420.
48 E. S. Shibu, K. Kimura and T. Pradeep, *Chem. Mater.*, 2009, **21**, 3773.
49 A. M. Kalsin, A. O. Pinchuk, S. K. Smoukov, M. Paszewski, G. C. Schatz and B. A. Grzybowski, *Nano Lett.*, 2006, **6**, 1896.
50 S. M. Rupich, E. V. Shevchenko, M. I. Bodnarchuk, B. Lee and D. V. Talapin, *J. Am. Chem. Soc.*, 2010, **132**, 289.
51 R. Q. Song and H. Cölfen, *Adv. Mater.*, 2010, **22**, 1301.
52 Y. H. Tseng, H. Y. Lin, M. H. Liu, Y. F. Chen and C. Y. Mou, *J. Phys. Chem. C*, 2009, **113**, 18053.
53 D. Schwahn, Y. R. Ma and H. Cölfen, *J. Phys. Chem. C*, 2007, **111**, 3224.
54 Y. Oaki and H. Imai, *Cryst. Growth Des.*, 2003, **3**, 711.
55 A. N. Kulak, P. Iddon, Y. T. Li, S. P. Armes, H. Cölfen, O. Paris, R. M. Wilson and F. C. Meldrum, *J. Am. Chem. Soc.*, 2007, **129**, 3729.
56 J. X. Fang, B. J. Ding and X. P. Song, *Cryst. Growth Des.*, 2008, **8**, 3616.
57 Z. L. Wang, *J. Phys. Chem. B*, 2000, **114**, 1153.
58 B. D. Wood, V. Mocanu and B. D. Gates, *Adv. Mater.*, 2008, **20**, 4552.
59 J. X. Fang, S. Y. Du, Z. Y. Li, S. Lebedkin, R. Kruk and H. Hahn, *Nano Lett.*, 2010, **10**, 5006.
60 J. W. Bai, Y. Qin, C. Y. Jiang and L. M. Qi, *Chem. Mater.*, 2007, **19**, 3367.
61 B. Lim, X. M. Lu, M. J. Jiang, P. H. C. Camargo, E. C. Cho, E. P. Lee and Y. N. Xia, *Nano Lett.*, 2008, **8**, 4043.
62 X. W. Teng, S. Maksimuk, S. Frommer and H. Yang, *Chem. Mater.*, 2007, **19**, 36.
63 M. Nogami, R. Koike, R. Jalem, G. Kawamura, Y. Yang and Y. Sasaki, *J. Phys. Chem. Lett.*, 2010, **1**, 568.
64 Y. G. Sun and G. P. Wiederrecht, *Small*, 2007, **3**, 1964.
65 Y. J. Song, Y. Yang, C. J. Medforth, E. Pereira, A. K. Singh, H. F. Xu, Y. B. Jiang, C. J. Brinker, F. Van Swol and J. A. Shelnutt, *J. Am. Chem. Soc.*, 2004, **126**, 635.
66 J. F. Ye, W. Liu, J. G. Cai, S. Chen, X. W. Zhao, H. H. Zhou and L. M. Qi, *J. Am. Chem. Soc.*, 2011, **133**, 933.
67 Z. Liu, X. D. Wen, X. L. Wu, Y. J. Gao, H. T. Chen, J. Zhu and P. K. Chu, *J. Am. Chem. Soc.*, 2009, **131**, 9405.
68 X. L. Wu, S. J. Xiong, Z. Liu, J. Chen, J. C. Shen, T. H. Li, P. H. Wu and P. K. Chu, *Nat. Nanotechnol.*, 2011, **6**, 103.
69 H. Wang and N. J. Halas, *Adv. Mater.*, 2008, **20**, 820–825.
70 H. Y. Liang, Z. P. Li, W. Z. Wang, Y. S. Wu and H. X. Xu, *Adv. Mater.*, 2009, **21**, 4614–4618.

